

Vibrations in the Turning Process and the Curves Diagram Over the Establishment of Stability

Ahmet Latifi*, Ismet Ibishi, Arsim Abazi, Astrit Shartari

University of Mitrovica, Faculty of Mechanical & Computer Engineering, Mitrovica, Kosova

Received December 17, 2016; Accepted February 16, 2017

Abstract: During processing by sliver removal, some vibrations occur as a result of force occurrence which belong to the variable character and which depend on physical essence and caused vibrations mechanisms. The vibrations appearance, their amplitude and frequency depend on the ratio between the caused forces and the characteristics of the flexible system in the machine, respectively into the system machine-workpiece and cutting tool. The Curves diagrams of stability, determine the level of stability in the turning operations.

Key words: Vibrations, stability curve diagrams, turning Machine, cutting tool.

Introduction

Meaning of vibrations is one of the meanings which mostly belong to the machine dynamics. Turning operations, especially operations for internal processing, are facing the difficult problem of vibrations. The reduction of vibrations requires extra care because this consists on planning of processing, respectively production associated with the preparation of a work piece in order to get the desired shape within the tolerated level. So the vibration problem on cutting metals has significant impact on factors such as productivity, manufacturing cost etc. only a detailed study on vibrations would be an important step on dealing with this problem.

The Vibration impact on the turning process

Vibrations in the turning process occur as result of the instability during the process if metal cutting. This phenomenon is characterized by violent vibrations, loud noise, and poor quality in the final surface. However, today there are identified at least two types of vibrations in the manufacturing process, forced and self excited. Loud acoustic noise in the work environment often occurs as a result of the dynamic movement between the cutting tool and the processing work piece. To begin, let's consider the tool and workpiece to be rigid and develop expressions for the cutting force, F . Figure 2. shows an "orthogonal cutting" operation, where only the normal, F_n , and tangential, F_t , components of the force are considered. In general, the cutting force vector includes the third component along the part axis, but the orthogonal treatment is sufficient for us to describe the process dynamics.



Figure 1. The vibration impact on the workpiece machining

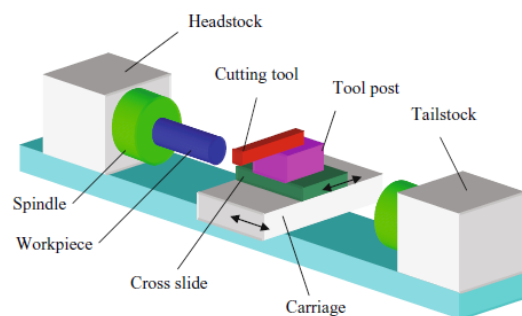


Figure 2. Schematic of manual lathe

Stability curves diagrams

Depending on the feedback system "gain", or chip width b , and spindle speed, Ω , the turning operation will either be stable or exhibit chatter (unstable cutting), which causes large vibrations and forces and leads to poor surface finish and, potentially, tool/workpiece damage. In stable machining,

*Corresponding: E-Mail:ahmet.latifi@umib.net; Tel: +377 44 192 250;

the vibrations diminish from revolution to revolution. In unstable machining, the vibrations grow from revolution to revolution until limited in some way. The governing relationships for this behavior are provided in Eqs. 1 through 3.

$$b_{lim} = \frac{-1}{2K_s \cos(\beta) \text{Re}[FRF]} \quad (1)$$

$$\frac{f_c}{\Omega} = N + \frac{\varepsilon}{2\pi} \quad (2)$$

$$\varepsilon = 2\pi - 2 \tan^{-1} \left(\frac{\text{Re}[FRF]}{\text{Im}[FRF]} \right) \quad (3)$$

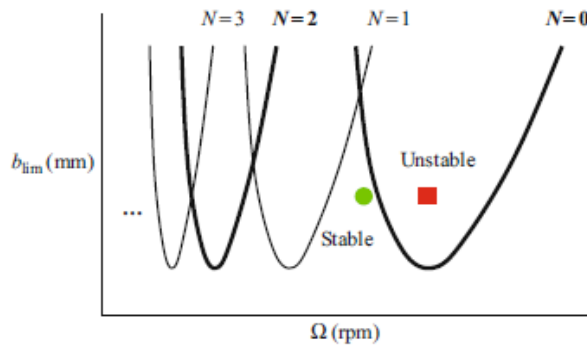


Figure 3. Example stability lobe diagram. The stability boundary separates stable chip widthspindle speed combinations (below the boundary, marked as a circle) from unstable pairs (above, marked as a square)

Figure 3 shows an example stability lobe diagram where the Ω versus b_{lim} family of curves ($N = 0, 1, 2, \dots$) separate the space into two regions. To explore the value of b as a function of kn and the tool vibrations, let's consider a unit value of the variable force, or $1 = k_n b(y(t-\tau) - y(t))$ from Eq. 4. This equation can be solved for b :

$$F_n = k_n b h(t) = k_n b (h_m + y(t-\tau) - y(t)) \quad (4)$$

$$b = \frac{1}{(k_n (y(t-\tau) - y(t)))} \quad (5)$$

Equation 6 shows the new relationship, where the negative sign is included in order to obtain positive (limiting) chip width values.

$$b_{\downarrow} \lim = \frac{(-1)}{(k_{\downarrow} n (2 \text{Re}[FRF]))} \quad (6)$$

Setting examples of stability in process of turning

Example 1. Competing lobes for two degree of freedom oriented FRF. Consider the model shown in Figure 4.

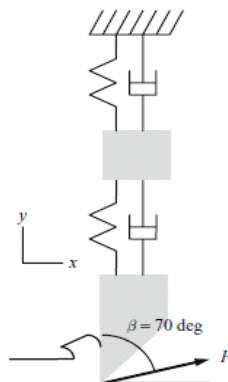


Figure 4. Two degree of freedom model for turning stability evaluation

A two degree of freedom system is aligned with the surface normal and the force angle is 70° . The directional orientation factor therefore only requires the projection of the force into the mode direction, $\mu = \cos(70)$.

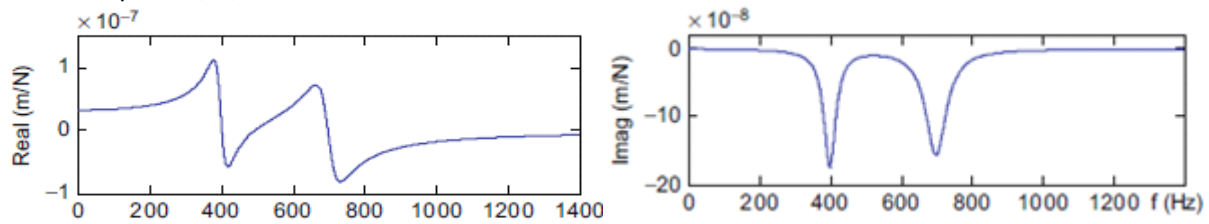


Figure 5. Real and imaginary part of the oriented FRF for the system

The modal parameters are: $f_{n1} = 400$ Hz, $k_{q1} = 2 \times 10^7$ N/m, $f_{n2} = 700$ Hz, $k_{q2} = 2.2 \times 10^7$ N/m, $\zeta = 0.5$. We will determine the stability behavior for this turning operation. The real and imaginary parts of the oriented FRF for this system are shown in Figure 5. Two distinct modes with 400 Hz and 700 Hz natural frequencies are observed. They occur where the real part is less than zero and are pictured in the top panel of Figure 6.

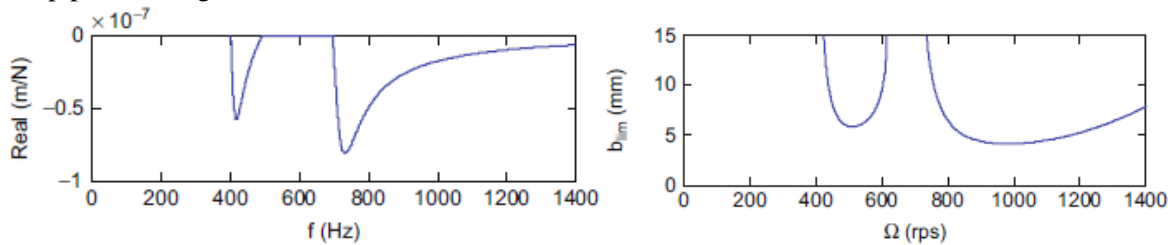


Figure 6. (a) Negative real part of oriented FRF. (b) Corresponding $N=0$, stability limit. The two lobes sections are present due to the two portions of the negative real part in the top panel.

In the bottom panel, the Ω and b_{lim} values, which are both a function of the FRF and therefore the chatter frequency (as seen in Eqs. 1-3), are plotted against one another to define the stability limit ($K_s = 1500$ N/mm²). It is seen that a distinct lobe section is associated with each of the two chatter frequency ranges. Only the $N=0$ pair is shown in this figure. However, it is the whole family of curves, $N=0, 1, 2, \dots$, that defines the overall stability boundary. The $N=0, 1$, and 2 lobes are shown in Figure 7.

Because these lobes can interfere with each other and limit the stable chip width, they may be considered as “competing lobes”. For example, it is seen that the right portion of the $N = 2$ lobe (corresponding to the 700 Hz mode) truncates the stable zone between the left (400 Hz mode) and right portions of the $N = 1$ lobe near 2000 rpm.

Example 2: Turning model with modes in two perpendicular directions. We’ll next determine the stability for the model in Fig. 8 with the following parameters: $\alpha_1 = 30^\circ$, $\alpha_2 = 60^\circ$, $\beta = 70^\circ$ dhe $K_s = 2000$ N/mm². The dynamics are defined by $f_{n1} = 421$ Hz, $k_1 = 2.8 \times 10^7$ N/m dhe $\zeta_1 = 0.05$ direction u_1 and $f_{n2} = 491$ Hz, $k_2 = 3.81 \times 10^7$ N/m and $\zeta_2 = 0.05$ for the u_2 direction.

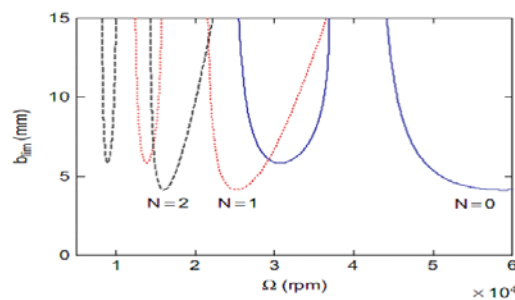


Figure 7. Competing $N=0, 1$ and 2 stability lobes for two degree of freedom system

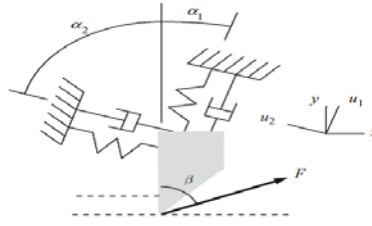


Figure 8. Turning model with a single degree of freedom in both the u1 and u2 directions.

$$\mu_1 = \cos(\beta - \alpha_1)\cos(\alpha_1) = \cos(70 - 30)\cos(30) = 0.663$$

$$\mu_2 = \cos(\beta - \alpha_2)\cos(\alpha_2) = \cos(70 + 60)\cos(60) = -0.321$$

The oriented FRF, as well as its components $\mu_1 FRF_{u1}$ and $\mu_2 FRF_{u2}$, are shown in Fig. 9. It is seen that: 1) the minimum real part of FRForient occurs at 443 Hz with a value of 1.493×10^{-4} mm/N; and 2) the real part crosses through zero amplitude at a frequency of 418 Hz (which corresponds to the natural frequency for a single degree of freedom system). Although this is not a single degree of freedom system, the real part of the oriented FRF bears some similarity to a single degree of freedom FRF real part. The best and worst spindle speeds are summarized in Table 1.

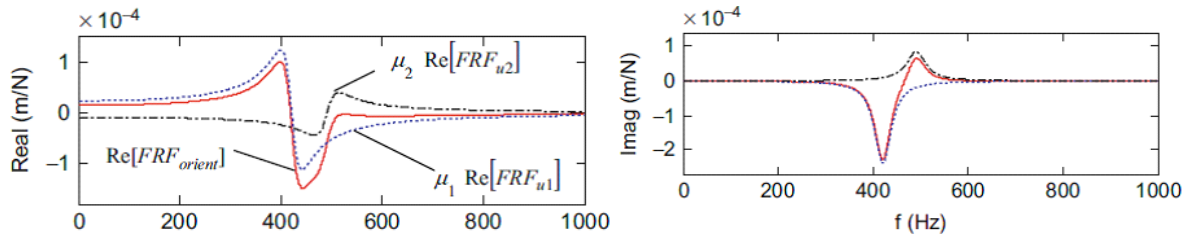


Figure 9. Oriented FRF for Ex1. The two components of the oriented FRF are also shown.

Table 1. Approximate best and worst spindle speeds for ex.1

no.	Ω_{best} (rps)	Ω_{best} (rpm)	Ω_{worst} (rps)	Ω_{worst} (rpm)
#1	209	12540	253	15180
#2	139	8340	161	9665
#3	105	6300	118	7088

$$b_{lim,crit} = \frac{-1}{2K_s \min(\text{Re}[FRF_{orient}])} = \frac{-1}{2 \cdot 200^0 (-1.493 \times 10^{-4})} = 1.7 \text{ mm}$$

$$\Omega_{keq} = \frac{418}{N+1} (\text{rps})$$

$$\Omega_{mir\ddot{e}} = \frac{443}{N + \frac{3}{4}} (\text{rps})$$

Figure 10 shows one valid chatter frequency range associated with the oriented FRF. As before, it occurs where the real part is less than zero (top panel). In the bottom panel, the $N = 0$ Ω and b_{lim} values are plotted against one another to define the stability limit. It is seen that the best speed of 418 rpm is a reasonable approximation of the actual behavior. Figure 11 shows the combined stability boundary for $N = 0$ to 3.

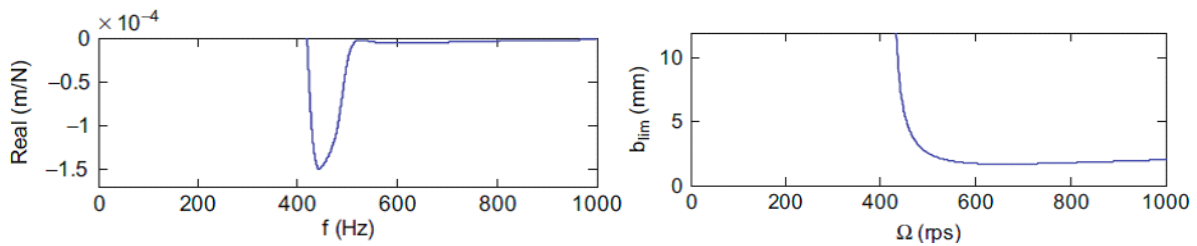


Figure 10. (a) Negative real part of oriented FRF for ex.2 (b) Corresponding $n=0$ stability limit

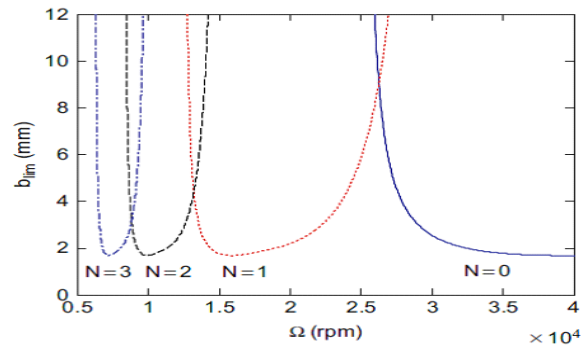


Figure 11. Stability lobes for ex.2 ($n=0$ to 3)

Conclusion

Whether we know it or not, whether we like it or not, every cutting operation has a picture like the one shown in Fig. 3. If we choose the cutting conditions at random, or at least without considering the applicable stability lobe diagram, then we sometimes choose stable cutting and sometimes not. Sometimes speeding up helps and other times it makes things worse. It appears to be random and many machine shops struggle with this issue every day. If we have the diagram and choose the cutting conditions accordingly, then it is possible to avoid the unstable conditions (chatter) and increase productivity.

References

- Abazi A, (2016) *Ndikimi I vibrimeve ne ashperesine e siperfaqeve te punuara gjate tornimit*. Msc. Thesis University of Prishtina, Prishtina/Kosovo.
- Thomson W, Dahleh M, (1998) *Theory of vibration with Application.*, 5th ed. Prentice Hall. Upper Saddle River, NJ.
- Weaver Jr.W, Timoshenko S, Young D, (1990) *Vibration problems in engineering* 5th Ed. John Wiley & Sons, New York.
- Tony LS, Smith KS, (2009) *Machining Dynamics*, New York.
- Zuperl U, Cus F, (2015) Simulation and visual control of chip size for constant surface roughness. *Int. J. Simulation Modelling* **14**, 392-403.